Nonlocal order in elongated dipolar gases

J. Ruhman,[1] E. G. Dalla Torre,[1,2] S. D. Huber,[1] and E. Altman[1]
[1]*Department of Condensed Matter Physics, Weizmann Institute of Science, Rehovot 76100, Israel*
[2]*Department of Physics, Harvard University, Cambridge Massachusetts 02138, USA*
(Received 7 November 2011; published 22 March 2012)

Dipolar particles in an elongated trap are expected to undergo a quantum phase transition from a linear to a zigzag structure with decreasing transverse confinement. We derive the low-energy effective theory of the transition showing that in the presence of quantum fluctuations the zigzag phase can be characterized by a long-ranged string order, while the local Ising correlations decay as a power law. This is also confirmed using density matrix renormalization group calculations on a microscopic model. The nonlocal order in the bulk gives rise to zero energy states localized at the interface between the ordered and disordered phases. Such an interface naturally arises when the particles are subject to a weak harmonic confinement along the tube axis. We compute the signature of the edge states in the single-particle tunneling spectra pointing to differences between a system with bosonic versus fermionic particles. Finally we assess the magnitude of the relevant quantum fluctuations in realistic systems of dipolar particles, including ultracold polar molecules as well as alkali atoms weakly dressed by a Rydberg excitation.

DOI: 10.1103/PhysRevB.85.125121 PACS number(s): 64.70.−p, 75.40.Mg, 61.66.−f, 71.10.Pm

I. INTRODUCTION

The realization of ultracold dipolar gases opens new directions for investigation of quantum many body physics. Relevant systems currently under investigation include degenerate gases of atoms with large magnetic dipole moments, such as Cr[1] or of heteronuclear molecules with a large permanent electric dipole.[2] Another promising proposal is to use degenerate alkali atoms which are weakly dressed with a Rydberg excitation by optical pumping.[3]

The long-range dipolar interactions in these systems can be strong enough to drive interesting structural phase transitions. But, not so strong as to make the kinetic energy negligible. The balance between kinetic and interaction terms results in strong quantum fluctuations, which provide a fertile ground for the formation of novel phases.[4,5]

In this paper we shall specifically consider the zigzag instability of a chain of repulsive particles in an elongated trap, shown schematically in Fig. 1. The dipoles are assumed to be polarized by an external electric field perpendicular to the trap axis. When the transverse confinement is lowered below a critical value, the repulsive interactions between dipoles overcome the confinement, leading to a staggered distortion of the chain. A classical analysis along these lines[6] explains the zigzag distortion observed in chains of trapped ions.[7] In the classical description of either the Coulomb or dipolar crystal, the zigzag distortion is associated with breaking of the $\mathbb{Z}_2$ reflection symmetry about the midplane of the trap. However, because the dipolar interactions are much weaker, the effect of quantum fluctuations in the particle positions is greatly enhanced compared to the ions. We shall see that this leads to an interesting change of the zigzag phase and phase transition.

One effect of quantum fluctuations is to allow single-particle tunneling between an up and down displacement in the zigzag. It is convenient to think of distortion of a particle, up or down as an Ising spin variable. The tunneling then acts to disorder the zigzag in the same way that a transverse field acts to disorder a one-dimensional Ising model inducing transitions between the up and down state of the spin. This class of fluctuations and a mapping to an Ising model were recently discussed.[8,9]

Another mode of quantum fluctuation, which has not been considered in this context so far, is the axial motion of the dipolar particles. In one dimension these longitudinal fluctuations lead to disordering of the crystal and at the same time they restore the $\mathbb{Z}_2$ symmetry of the staggered configuration. What is then the fate of the phase transition and of the broken symmetry phase in the presence of the fluctuations?

To answer this question we derive a long wavelength theory, which describes both the gapless longitudinal fluctuations and the transverse distortion. Let us briefly summarize the main results of this analysis. First, we show that the zigzag state remains a distinct phase in the presence of the fluctuations, however, the zigzag order becomes nonlocal and is described by a string order parameter. The longitudinal density fluctuations (breathing modes of the zigzag) remain gapless in the zigzag phase, while single-particle excitations induce domain walls in the string order and are therefore gapped. We further show that the presence of string order in the bulk implies the existence of a zero energy single-particle state localized at each edge. These states are represented by localized Majorana modes in the low-energy theory. We compute the local tunneling spectra into the edge and identify the signatures of the localized zero energy states. Finally we point to interesting differences in these signatures depending on whether the dipolar particles are of a bosonic or a fermionic species.

Before proceeding we note previous analysis done in the context of electronic quantum wires,[10–12] which also identify a quantum phase transition, of the same universality class as we consider here, into a zigzag chain. While the nonlocal nature of the order parameter is implicit in these studies, this nonlocality has not been emphasized, and in particular its implications on the edge structure have not been discussed. We also note earlier studies on bosonic[13] and fermionic[14,15] ladders, where a state similar to the zigzag is identified as an out of phase charge density wave between the two legs of the ladder.

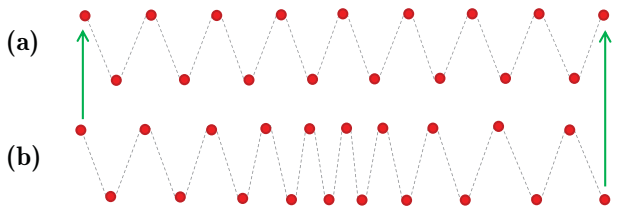

FIG. 1. (Color online) (a) One of the two broken symmetry zigzag states of the classical system. (b) Longitudinal quantum fluctuations affect a continuous distortion from one zigzag configuration to the other, which restores the $\mathbb{Z}_2$ symmetry of the ground state in the bulk.

The rest of the paper is organized as follows. In Sec. II we identify the important scales in the problem of dipolar particles in an elongated trap and derive an effective Hamiltonian of the particles in first quantized form. A quantum mean-field approximation is then formulated in Sec. III in order to estimate the transition point and assess the importance of quantum fluctuations within the interaction range relevant to ultracold dipolar molecules or Rydberg atoms. In Sec. IV we derive an effective long-wavelength theory of the zigzag transition starting from the microscopic Hamiltonian of the dipolar chain. Using the long-wave description we discuss the nature of the critical point and the nonlocal order parameter associated with the zigzag phase. The low energy edge states imposed by the nonlocal order in the bulk are discussed in Sec. V. In particular we predict direct signatures of the zero energy edge states in local tunneling spectra. In Sec. VI we demonstrate the key properties of the zigzag chain, in particular the presence of string order, in a numerical calculation using the density matrix renormalization group (DMRG) method. Finally, Sec. VII provides a summary and discussion of the results.

II. MODEL HAMILTONIAN

We consider a dipolar quantum gas tightly confined in a tube-shaped trapping potential. The particles of the gas may be either fermionic or bosonic and we assume that their dipoles are polarized by a large electric field (or magnetic field in the case of atoms with a large magnetic dipole moment) in the direction $\hat{\mathbf{z}}$ perpendicular to the tube axis. Such a setup is described by the Hamiltonian,

$$H = \sum_i \left(\frac{P_i^2}{2m} + \frac{m\omega_\perp^2}{2} r_i^2 \right) + d^2 \sum_{j>i} \left(\frac{1}{|\mathbf{R}_i - \mathbf{R}_j|^3} - 3\frac{((\mathbf{R}_i - \mathbf{R}_j)\cdot\hat{\mathbf{z}})^2}{|\mathbf{R}_i - \mathbf{R}_j|^5} \right), \quad (1)$$

where $\mathbf{P}_i$, $\mathbf{R}_i$, and r_i are the first quantized momenta, position, and transverse radial coordinates of the particles in the trap. $\omega_\perp$ is the transverse harmonic confinement frequency m is the mass and d the dipole moment of the particles.

A simple way to analyze the Hamiltonian (1) is through a classical mean-field theory. This approach consists of minimizing the potential energy while neglecting the kinetic terms that induce fluctuation in the positions. A zigzag transition is captured by a Landau-like expansion of the configuration energy in powers of the staggered distortion r of the particles.[6] For transverse confinement frequency $\omega_\perp$ below the critical frequency $\omega_c = \sqrt{279\zeta(5) d^2 \rho_0^5/8m}$, the classical energy is minimized by a nonvanishing distortion $r = \kappa\, \rho_0^{-1}\sqrt{1-(\omega_\perp/\omega_c)^2}$, where $\kappa = \sqrt{186\zeta(5)/3175\zeta(7)} \approx 0.245$, $\zeta(n)$ is the Riemann zeta function, and ρ_0 is the particle density. In reality, this criterion only marks the characteristic frequency around which a local zigzag distortion begins to develop. Quantum fluctuations allow the zigzag to twist and turn and may ultimately destroy the long-range order.

To describe the soft fluctuations of the zigzag we assume that each particle is distorted off the axis of the trap by the fixed classical value r, but is free to rotate around the axis by the angle φ. All our expansions below are valid when the distortion r is small compared to the interparticle distance, that is, $\tilde{r} \equiv r\rho_0$ should be taken to be a small dimensionless parameter. In Sec. III we will see that in the relevant range of parameters for dipolar molecules this is always satisfied near the zigzag quantum phase transition.

The effective Hamiltonian which describes the linear motion of particles along the trap axis, rotations around the axis at a fixed radius r, and dipolar interactions between particles is given by

$$H = \sum_i \left[\frac{p_i^2}{2m} + \sum_{j>i} \frac{d^2}{|x_i - x_j|^3} + \frac{L_i^2}{2I} + \sum_{j>i} J_{ij} \left(\cos(\varphi_i - \varphi_j) + \frac{1}{2}\cos(\varphi_i + \varphi_j) - \frac{\nu}{2}\cos 2\varphi_i \right) \right]. \quad (2)$$

Here p_i and x_i are the linear momenta and position operators and L_i and φ_i are the angular momenta (along the axis) and its conjugate angle operator of the ith particle. The first two terms in the Hamiltonian (2) describe the particle motion and interactions along the trap axis, which give rise to density fluctuations. The rest of the Hamiltonian describes the fluctuations that drive the Ising transition. Apart from the last term, the angular part of the Hamiltonian looks like a quantum xy model. The dipolar interaction, through the cosine coupling favors a staggered arrangement of the molecules off the axis, while the angular kinetic energy delocalizes the angle and thereby acts to disorder the zigzag. The last term breaks the $U(1)$ angle symmetry down to $\mathbb{Z}_2$ by favoring the up and down (0 and π) distortions of the particles. If the trap potential has cylindrical symmetry then the preferred axis is set only by the external electric field which polarizes the dipoles. In this case we have $\nu = 1$. It is possible to change ν by tuning the ratio between the transverse trap frequencies parallel and perpendicular to the electric field.

The other coupling constants appearing in the effective Hamiltonian (2) are calculated directly from the full Hamiltonian (1). They are given by $J_{ij} = J/(\rho_0|x_i - x_j|)^5$ where $J = 6d^2r^2\rho_0^5$ and $I = mr^2$. Note that the strength of the coupling J_{ij} depends on the particles' positions such that it produces a coupling between the angular and longitudinal degrees of freedom. At this point it is convenient to express J and I in terms of two important dimensionless parameters that can be independently tuned in the system: (i) $\tilde{r} \equiv r\rho_0$ is the ratio of the classical distortion radius to the average interparticle distance, and (ii) the dimensionless dipolar interaction strength $R_s = d^2\rho_0 m/\hbar^2$ is the ratio of the typical dipolar energy $\epsilon_d = d^2\rho_0^3$

to the typical kinetic energy $\epsilon_0 = \hbar^2\rho_0^2/m$. R_s can be varied, for example, by changing the dipole moment d using an external electric field, while $\tilde{r}$ is tuned by varying the transverse trap frequency $\omega_\perp$. We can express the Hamiltonian parameters using these dimensionless numbers as $J = 6R_s\tilde{r}^2\epsilon_0$ and $I = \hbar^2\tilde{r}^2/\epsilon_0$.

III. ESTIMATION OF THE TRANSITION POINT

Within a classical analysis[6] the zigzag transition takes place at a critical value of the transverse trap frequency given by $\omega_c = 6.014\sqrt{R_s}\epsilon_0/\hbar$. Quantum fluctuations driven by the kinetic energy in the Hamiltonian (1) or (2) will lead to a transition at a smaller value of the transverse trap frequency. With increasing strength of interaction R_s the relative importance of the kinetic energy decreases and we expect the critical $\omega_\perp$ to approach the classical value.

We shall now formulate a quantum mean-field theory of the effective Hamiltonian (2) in order to estimate the value of the parameters at the transition point and to asses the importance of quantum fluctuations. For this purpose we freeze the axial degrees of freedom and focus on the angular part of the Hamiltonian (2). In addition, since J_{ij} decays rapidly with distance, we consider only nearest neighbor interactions.

The mean-field approximation consists of decoupling the interaction term in the Hamiltonian (2) to get the local Hamiltonian,

$$H_{\rm MF} = \sum_i \left[\frac{L_i^2}{2I} - J\left(3\sigma\,\cos\varphi_i + \frac{\nu}{2}\cos 2\varphi_i\right)\right]. \qquad (3)$$

This is supplemented by the self-consistency condition,

$$\sigma = \langle\cos\varphi_i\rangle_{\rm MF}\,. \qquad (4)$$

Note that the Hamiltonian (3) is fully quantum mechanical in the sense that the noncommuting variables φ_i and L_i are both present in it, in the interaction and kinetic terms, respectively. Furthermore the transition is a result of competition between these two terms, and not driven by interaction alone as in the classical zigzag instability. On the other hand this local mean-field scheme neglects the spatial structure of the fluctuations and hence cannot capture the universal critical behavior close to the transition. Below we estimate the fluctuation region in which the mean-field theory fails.

Within the mean-field approximation, the system develops a nonzero order parameter σ at the critical value of the couplings $IJ = \alpha(\nu)$. For example, we find $\alpha(1) = 0.31$, $\alpha(0.5) = 0.33$, and $\alpha(2) = 0.28$. While larger values of the eccentricity can be achieved in experiment, our quantum rotor representation is not suited to describe them quantitatively.

Using the relations $IJ = 6R_s\tilde{r}^4$ and $\tilde{r} = \kappa\sqrt{1-(\omega_\perp/\omega_c)^2}$ we infer a phase boundary,

$$R_s^{\rm crit} = 46\,\alpha(\nu)\left[\frac{1}{1-(\omega_\perp/\omega_c)^2}\right]^2. \qquad (5)$$

The phase diagram is presented in Fig. 2 for the case of a symmetric trap ($\nu = 1$). We see that the transition point indeed approaches the classical value of ω_c in the strong interaction limit.[16] Reasonable values for the dimensionless interaction R_s expected in real systems can be estimated from

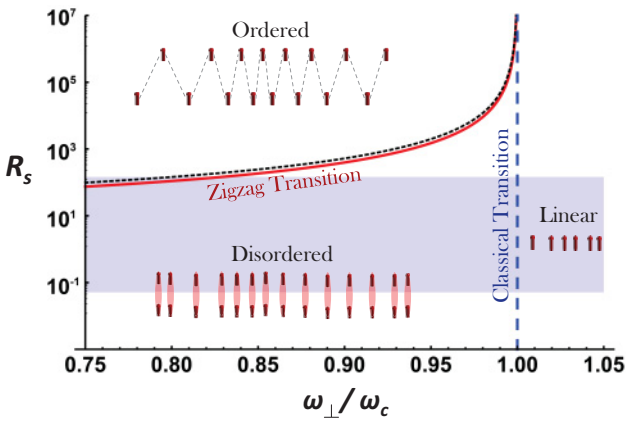

FIG. 2. (Color online) Phase diagram of polar molecules in an elongated trap in the space of the dimensionless interaction constant, $R_s = d^2m\rho_0$, and transverse confinement $\omega_\perp/\omega_c$, ω_c is the critical transverse frequency in the classical limit. The solid curve marks the zigzag transition (5) computed within the local mean-field approximation for $\nu = 1$, that is, for isotropic transverse confinement. The dashed line corresponds to the Ginzburg criterion below which we expect the mean-field approximation to break down. Realistic values of R_s range between 0.05 and 130 as marked by the gray band. Note that the quantum disordered zigzag and the linear chain are not sharply distinct. There is a smooth crossover between the two regimes.

the typical dipolar moments ranging from $d \simeq 0.05$ D for magnetic moments through $d \simeq 0.5$ D for polarized molecules and up to $d \simeq 10$ D for atoms weakly dressed with Rydberg excitations. Assuming densities of $\rho_0 \sim 10^4\,{\rm cm}^{-1}$, we get R_s between 0.05 and 130. From the phase diagram (Fig. 2) it is clear that in this regime quantum fluctuations shift the transition to $\omega_\perp^{QC}$ far below the classical value ω_c. This implies a huge effect of quantum fluctuations on the transition in the relevant parameter regime.

We assess the accuracy of the quantum mean-field approximation used to compute the transition point by applying the appropriate Ginzburg criterion $\langle\delta\sigma^2\rangle/\langle\sigma\rangle^2 \sim 1$. The shift of the mean-field transition line from the line on which the Ginzburg criterion is satisfied (black short-dashed line in Fig. 2) estimates the error in determination of the critical point. In terms of the dimensionless coupling $\alpha = IJ$ the Ginzburg criterion is satisfied at $\alpha \approx 0.4$ (for $\nu = 1$) compared to the mean-field transition found at $\alpha = 0.31$.

IV. LONG WAVELENGTH THEORY

To capture the universal properties of the zigzag transition and the effects of the low-energy longitudinal fluctuations, we derive an effective long wavelength description of the Hamiltonian (2). The longitudinal modes are treated in a standard way. We replace the particle position x_j with the smooth displacement field $\phi_\rho(x_j)$ and the particle momenta by the conjugate field $\frac{1}{\pi}\partial_x\theta_\rho(x_j)$. These replacements allow one to take the continuum limit of the first line in Eq. (2) to obtain

$$\mathcal{H}_\rho = \frac{\hbar\,u_\rho}{2\pi}\int dx\left[K_\rho(\partial_x\theta_\rho)^2 + \frac{1}{K_\rho}(\partial_x\phi_\rho)^2\right], \qquad (6)$$

where $K_\rho = \pi/\sqrt{12R_s}$ and $u_\rho = \sqrt{12R_s}(\hbar\rho_0/m)$. From here on we rescale the coordinate x by the interparticle distance ρ_0^{-1} and rescale energies by the typical kinetic energy $\epsilon_0 = \hbar^2\rho_0^2/m$. After this transformation the velocity becomes dimensionless $u_\rho = \sqrt{12R_s}$.

The long wavelength limit of the angular Hamiltonian should be taken with more care. Because the angle φ_i has a staggered arrangement it cannot be directly replaced by a continuum field $\varphi(x_i)$. Instead we must make a staggered transformation,

$$\phi_{\sigma,i} = (\varphi_i + \pi N_i) \bmod 2\pi, \tag{7}$$

where $N_i = \sum_j \Theta(x_i - x_j)$ counts the number of particles to the left of the ith particle. Thus the new variable is slowly varying in space, with the price of being a nonlocal operator. Now we take the continuum limit through the substitution $\phi_{\sigma,j} \to \phi_\sigma(x_j)$ and $L_j \to \frac{1}{\pi\rho_0}\partial_x\theta_\sigma(x_j)$. In addition, noting that $N_i \to \pi\rho_0 x - \phi_\rho(x)$ we can express the original local Ising distortion as a composite of the two slowly varying fields $\hat\sigma(x) = r\cos(\varphi(x)) = r\cos(\phi_\sigma(x) + \phi_\rho(x) - \pi\rho_0 x)$.

The long wavelength Hamiltonian in the angular sector, including only the most relevant terms, is given by

$$\mathcal{H}_\sigma = \frac{u_\sigma}{2\pi}\int dx\left[K_\sigma(\partial_x\theta_\sigma)^2 + \frac{1}{K_\sigma}(\partial_x\phi_\sigma)^2\right] + \int dx(-g_1\cos 2\phi_\sigma + g_2\cos 2\theta_\sigma), \tag{8}$$

$$\mathcal{H}_c = -\lambda\frac{2\rho_0}{\pi^2}\int dx\,\partial_x\phi_\rho(1-\cos 2\phi_\sigma). \tag{9}$$

Here again we have rescaled the coordinate $x \to x\rho_0$ and energies $\epsilon \to \epsilon/\epsilon_0$ in order to work with dimensionless coefficients. The term g_1 originates directly from the last term in Eq. (2), from which its (bare) value can be estimated to be $g_1 = J = 6R_s\tilde r^2$. The term g_2 accounts for the compactness of the original angle variable. The value of the coefficient is the fugacity of kink-anti-kink pairs in ϕ_σ. It is estimated from the action associated with tunneling between the two potential minima $\phi_\sigma = 0$ and π through the barrier $J\cos 2\theta_\sigma$.[17] Within the WKB approximation we obtain $g_2 \approx I^{-1}\,e^{-8\sqrt{IJ}} = \tilde r^{-2}\exp(-8\sqrt{R_s\tilde r^4})$. In addition, we extract from (2) the bare value of the Luttinger parameter $K_\sigma^{-1} = \pi\sqrt{IJ} = \pi\sqrt{6\tilde r^4 R_s}$ and the velocity $u_\sigma = u_\rho/\sqrt{2} = \sqrt{6R_s}$.

Finally the term (9) describes the coupling between the longitudinal phonons and the zigzag degrees of freedom. It is generated because the energy gain associated with a zigzag arrangement, proportional to J_{ij}, is modulated with the distance $x_i - x_j$ between neighboring atoms along the chain. The field $\partial_x\phi$ which couples to the zigzag energy in (9) is simply the long wavelength limit of $x_i - x_j$. The value of the coupling constant is again extracted directly from (2), $\lambda = 15\pi R_s\tilde r^2$. Other coupling terms between the two sectors have been omitted since they turn out to have lower scaling dimension at the critical point which describes the zigzag transition.

We note that our derivation of the field theory was carried out in the strongly interacting limit $R_s \gg 1$, where the particles almost form a Wigner crystal. In this case the low-energy Hamiltonian is essentially independent of the statistics (bosonic or fermionic) of the constituent particles. As we shall see later, the differences due to particle statistics arise when we try to probe the system by inserting or extracting single particles to it.

Having derived the effective field theory we are now in a position to discuss the resulting quantum phases and phase transitions. Let us start with the phases. The Hamiltonian $\mathcal{H}_\sigma$ of the angular degrees of freedom describes a competition between two cosine terms in a regime where they are both relevant with respect to the quadratic part of the Hamiltonian. In the zigzag ordered phase the term g_1 is dominant. The field ϕ_σ is then pinned to one of the two minima at 0 or π, and the Ising-like order parameter $\langle\cos\phi_\sigma(x)\rangle$ takes a nonvanishing value $+1$ or -1. On the other hand when g_2 becomes dominant the dual variable θ_σ is pinned, leading to proliferation of phase slips in ϕ_s and disordering of the Ising field.

The representation of the order parameter in terms of the bosonic field ϕ_σ conceals the fact that the order in the zigzag phase is nonlocal. It consists of an infinite string operator when written in terms of the actual particle distortion $\hat\sigma(x) = r\cos\varphi(x)$,

$$\langle r\cos\phi_\sigma(x)\rangle = \left\langle e^{i\pi\int_{-\infty}^{x}\rho(x')\,dx'}\hat\sigma(x)\right\rangle, \tag{10}$$

where $\rho(x)$ is the particle density. The string order parameter captures the fact that the phase of the zigzag, namely an up or down distortion, is alternating in the particle frame but is not fixed to a position in the laboratory frame. The direct correlation function of the transverse distortions $\hat\sigma(x) = r\cos\varphi(x)$ decays as a power law along the chain due to disordering of the positional order:

$$\langle\hat\sigma(x)\hat\sigma(0)\rangle \to r^2\cos(\pi\rho_0 x)\langle\cos\phi_\sigma\rangle^2|x|^{-K_\rho}. \tag{11}$$

Let us move on to discuss the critical point separating the zigzag from the disordered phase. If we ignore for the moment the coupling λ between the zigzag degrees of freedom and the longitudinal phonons, then by symmetry considerations the effective Hamiltonian (8) is expected to describe an Ising critical point. When $K_\sigma = 1$ the problem becomes particularly simple, since we can immediately express $\mathcal{H}_\sigma$ as a model of two independent Majorana fermions or alternatively a single Dirac fermion:[18,19]

$$\mathcal{H}_\sigma = \int\sum_{\eta=\pm} dx\,\xi^\eta\left[-\mathrm{i}\frac{\tilde u_\sigma}{2}\,\partial_x\,\tau^z + \Delta_\eta\,\tau^y\right]\xi^\eta. \tag{12}$$

Here $\tilde u_\sigma = u_\sigma$, $\xi^\eta = (\xi_R^\eta, \xi_L^\eta)^T$ is a Majorana spinor in the chiral basis, and $\tau^{y,z}$ are Pauli matrices that act in this basis. The masses of the two Majorana modes are given by $\Delta_\pm = \pi(g_2 \pm g_1)$. The transition at $g_1 = g_2$ is then described by a single massless Majorana mode ξ^-, while the other gapped mode can be ignored. This is precisely the critical theory of the transverse field Ising model.[20] The relation between the low-energy Majorana mode and the bosonic fields in the low-energy limit is

$$\xi_R^- = -\sqrt{\rho_0/\pi}\,:\sin(\theta_\sigma - \phi_\sigma):\tag{13}$$

$$\xi_L^- = \sqrt{\rho_0/\pi}\,:\cos(\theta_\sigma + \phi_\sigma):\tag{14}$$

From the mean-field analysis presented in Sec. III we expect the transition to occur at a bare value of K_σ close to, but

not necessarily precisely, one. A deviation from $K_\sigma = 1$ (see Appendix A) gives rise to an interaction that couples the two sectors of Majorana fermions,

$$\mathcal{H}_\sigma^{(I)} = V \int dx\, \xi_R^- \xi_L^+ \xi_R^+ \xi_L^-, \tag{15}$$

where $V = 2\pi u_\sigma (K_\sigma^{-1} - K_\sigma)$. In addition, there is an increase in the velocity of the Majorana modes, which now becomes $\tilde{u}_\sigma = \frac{u_\sigma}{2}(K_\sigma^{-1} + K_\sigma)$.

Because the interaction couples the critical modes to a gapped excitation it is perturbatively irrelevant at the critical point. In other words the double sine-Gordon model (8) flows under renormalization to the self-dual (Ising) point $K_\sigma = 1$. The residual effect of the interaction is to shift the transition away from the point $g_1 = g_2$. This shift can be estimated using a mean-field decoupling of $\xi_R^- \xi_L^-$ from $\xi_L^+ \xi_R^+$ in Eq. (15). From here on we consider only the low-energy mode ξ^- and omit the $\eta = -$ superscript.

So far we have ignored the coupling λ between the Ising degrees of freedom and the longitudinal phonons. The effect of this coupling, which *a priori* breaks the conformal invariance and Lorentz symmetry of the Ising critical point, was addressed in Ref. 12 using a perturbative renormalization group analysis in λ. To one loop order, λ was found to be irrelevant if the sound velocity u_ρ is initially larger than the velocity of the Majorana mode $\tilde{u}_\sigma$. The slow flow toward $\lambda = 0$ has a peculiar effect on the fixed point. The ratio between the two velocities $\tilde{u}_\sigma / u_\rho$ approaches unity, thereby restoring Lorentz symmetry at the fixed point. However, at the same time the velocities themselves flow to zero. In the opposite regime, $\tilde{u}_\sigma > u_\rho$ the coupling λ is relevant. The nature of the transition in this case is not well understood and furthermore corrections beyond one loop can change the picture. We would like to point out, however, that a perturbative expansion in λ is justified for the bare values of the parameters dictated by our system. The small parameter of the expansion is $\lambda\sqrt{K_\rho/(\tilde{u}_\sigma u_\rho)}$, which in our case scales as $1/\sqrt{R_s} \ll 1$.

An experiment can in principle explore both of the above regimes by tuning the ratio $\tilde{u}_\sigma / u_\rho$. We have shown in Sec. III that changing the eccentricity of the transverse confinement leads to change of the critical value of $R_s \tilde{r}^2$ and therefore also of the bare Luttinger parameter K_σ near the transition point. For $K_\sigma = 1$ the ratio $\tilde{u}_\sigma / u_\rho = 1/\sqrt{2} < 1$, while by changing (bare) K_σ the ratio can be tuned above 1.

Finally, it is interesting to note the difference between our model of the zigzag transition and the problem of a two-leg fermion ladder discussed in Ref. 14. As we have mentioned above, such a fermion model should not be essentially different from ours in the strong interaction limit. However, Ref. 14 assumes the weak coupling perspective, taking the Fermi energy to be much larger than both the interaction and the splitting between the two sub-bands. This leads after bosonization (using our conventions) to a double sine-Gordon model similar to (8) in the "spin" (antisymmetric) sector, but with the term $g_2 \cos 2\theta$ replaced by a $\cos 4\theta$ term, which corresponds to Cooper pairing. Accordingly the phase competing with the zigzag in the weak coupling limit is a superconductor (i.e., quasi-long-range order in the pairing field), while in our case the competing phase is unpaired. The critical theory which describes the transition into the paired phase is different from the transition to the unpaired state found in our case. Note in particular that the self-dual point of the double sine-Gordon model with the pairing term is at $K_\sigma = 2$ rather than $K_\sigma = 1$ in our case.

V. ZERO ENERGY EDGE STATES

The nonlocal order has interesting consequences for the physics of the edge. Let us consider a physical model of the edge as an interface between the string-ordered zigzag phase and the disordered phase, created by a spatially dependent gap parameter $\Delta(x)$ that changes sign on the interface. This is in fact a realistic model for dipolar particles in a harmonic trap (see Fig. 3). The density which slowly decreases away from the center along the trap is a tuning parameter for the zigzag instability. Therefore, the dense middle section may be in the zigzag phase, the wings of the cloud are in the disordered phase, and there is necessarily an interface between the two regions.

The Hamiltonian (12) is formally identical to a one-dimensional superconductor of spinless fermions. This model has a zero-energy Majorana mode localized at the interface, where the gap function changes sign.[21] The zero mode has a particularly simple structure if Δ changes abruptly across the interface from Δ_0 to $-\Delta_0$ (see Appendix B). It is then given by the Majorana operator,

$$\gamma_0 = \sqrt{\frac{1}{2l}} \int dx\, e^{-\frac{|x|}{2l}} (\xi_L(x) + \xi_R(x)), \tag{16}$$

where $l = \tilde{u}_\sigma / 4\Delta_0$ is the correlation length. Bulk states of (12) are above the gap Δ_0.

Here we should remark on the difference between the Majorana edge modes of the zigzag phase and those found in two other one-dimensional systems. Consider first the transverse field Ising model. The representation of this model in terms of Jordan-Wigner fermions shows Majorana zero modes localized at the two edges. But when mapped back to

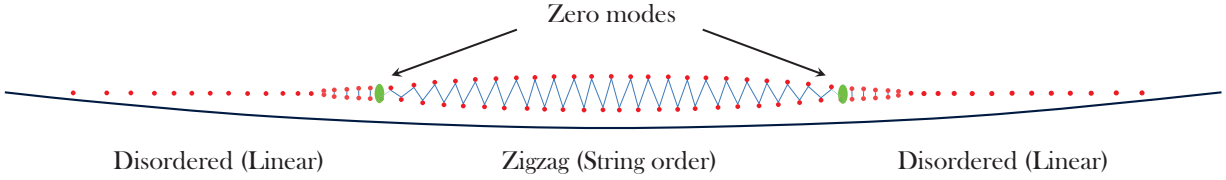

FIG. 3. (Color online) States of dipolar particles along an elongated trap with soft harmonic confinement. The inhomogeneous density along the trap acts as a tuning parameter of the zigzag transition. Here the particles in the dense middle section are in the zigzag phase while the wings of the cloud are in the disordered phase. Majorana zero modes are exponentially localized near the interfaces between the two phases.

the original Ising degrees of freedom, these two modes simply span the Hilbert space of the two broken symmetry states in the bulk. In our case, because there is no broken symmetry in the bulk the zero modes are truly localized at the edge, as we will show explicitly below.

There is also an important difference between the Majorana edge modes discussed here and those of a spinless fermion model in which the fermions are the local degrees of freedom. In our case, the Majorana modes appear only in the spin sector, where they describe a double degeneracy of the spectrum for a given charge parity of the zigzag. For even parity, the two states can be understood as either a zigzag that starts with an up distortion and ends down, or the opposite configuration. For odd parity the two states correspond to a zigzag with an up or down distortion at both ends. However, in a system with an interface, where the parity is not well defined, all four states should exist and may be combined into completely local excitations. This is in contrast to the nonlocal nature of the edge modes in the fermionic wire.[21]

We shall look for physical signatures of the edge states in the local tunneling density of states (DOS).[14] Consider a probe that can tunnel particles into or out of the system at a desired point x and energy ω. Such local probes have been proposed,[22] and are now becoming a reality in cold atomic systems.[23,24] We also assume that the position of the tunneling tip is asymmetric with respect to the tube axis so that it can insert a particle either displaced up or ($s = \uparrow$) down ($s = \downarrow$) in the tube. The tunneling rate is proportional to the local spectral function,

$$A_s(\omega,x) = \mathrm{Im}\left[\frac{\mathrm{i}}{\pi}\int dt\, \mathrm{e}^{\mathrm{i}\omega t}\Theta(t)\langle[\,\Psi_s(t,x)\,,\,\Psi_s^\dagger(0,x)\,]_\pm\rangle\right]. \tag{17}$$

where the $\pm$ subscript denotes anticommutator and commutator for fermions and bosons, respectively. To find the low-energy behavior of the spectral function we seek the representation of the particle field operators in terms of the bosonic density modes ϕ_ρ and θ_ρ and the low-energy Majorana fermion ξ. This will depend in a crucial way on the species, that is, bosonic or fermionic, of the dipolar particles. In what follows we separately treat each of these cases.

Bosonic particles. Let us start from the standard bosonization identity for bosonic particles in two chains labeled by $s = \uparrow(+), \downarrow(-)$,

$$\Psi^\dagger_{B,s} \simeq \sqrt{\rho_0} e^{-i\,\theta_s} \sum_{m=-\infty}^{\infty} e^{-i2m(\phi_s+\pi\rho_0 x)}. \tag{18}$$

We now canonically transform to a representation in terms of symmetric ("charge") and antisymmetric ("spin") fields through $\theta_s = \theta_\rho + s\,\theta_\sigma$ and $\phi_s = (\phi_\rho + s\,\phi_\sigma)/2$. Keeping the most relevant terms $m = 0, \pm 1$ and using the bosonized form (13) and (14) of the Majorana operators we obtain

$$\begin{aligned}\Psi^\dagger_{B,s} \simeq{}& \beta_0\sqrt{\rho_0}\, e^{-i\,\theta_\rho} e^{-i\,s\,\theta_\sigma} + \beta_1\, e^{-i\,\theta_\rho}(e^{i(\phi_\rho+2\pi\rho_0 x)}\,\xi_L \\ &- i\,s\; e^{-i(\phi_\rho+2\pi\rho_0 x)}\,\xi_R),\end{aligned} \tag{19}$$

where β_0 and β_1 are nonuniversal coefficients. The first row in the operator (19) corresponds to the long-wavelength components of the boson. The second row describes the components with wavelength comparable to the interparticle spacing. In both terms insertion of a boson must cause a disruption in the zigzag order. In the first case the operator $e^{\pm i\,\theta_\sigma}$ creates a kink in the Ising order parameter, while in the second case the disruption is affected by the Majorana operator.

Since we are interested in the low-energy contributions near the interface we can further simplify the Bose operator. First the factor $e^{\pm i\,\theta_\sigma}$ can be replaced by its expectation value, which decays exponentially with distance from the interface in the ordered side (recall that $\langle e^{i\,\theta_\sigma}\rangle$ is the "dual Ising order parameter"). Second, the Majorana operators $\xi_{L,R}$ can be replaced by the contribution to them from the zero energy edge mode, $\xi_{L,R} \sim e^{-\frac{2\Delta_0}{v}|x|}\gamma_0$. From here we can easily compute the local spectral function at low energies (see Appendix D):

$$A(E,x) \approx \left(\frac{B_0}{1+e^{x/l}} + B_1\, e^{-|x|/l}|E|^{K_\rho}\right)|E|^{\frac{1}{4K_\rho}-1}, \tag{20}$$

where $B_{0,1}$ are nonuniversal constants. The leading (first) term originates from the long wavelength contribution to the Bose operator. Only the subleading term B_1 stems from the Majorana zero mode.

Fermionic particles. Unlike with bosonic particles, we cannot access the zigzag phase of fermions starting from weakly coupled Luttinger liquids. A better starting point to obtain the low-energy limit of the fermion field is a two-band model, including the ground state and first transverse excitation in the tube.[10–12] Details of the formulation are left to Appendix C, however, the end result is simple. A fermion inserted into the lower band is described by

$$\psi_0^\dagger \simeq \alpha_0\sqrt{\rho_0}\sum_{r=R,L} e^{-i\,r k_F x} e^{i\,(r\phi_\rho-\theta_\rho)} e^{-i\,r\,\theta_\sigma}. \tag{21}$$

This is directly analogous to the first term in Eq. (19), except that the fermion is not inserted at zero momentum but rather at the Fermi points of the Luttinger liquid that describes the breathing modes of the zigzag. Insertion of a fermion must be accompanied by creation of a kink in the zigzag order, which is implemented by the factor $e^{\pm\mathrm{i}\,\theta_\sigma}$. Because on both sides of the transition there is a gap to a second band, the fermion can also be inserted at zero momentum above the gap. This "second band" fermion is directly proportional to the Majorana modes (see Appendix C):

$$\psi_1^\dagger \simeq \alpha_1\frac{e^{i\frac{\pi}{4}}}{\sqrt{2}}(\xi_R - i\,\xi_L)\,e^{-i\,\theta_\rho}. \tag{22}$$

A fermion distorted up or down in the tube is now described by a superposition of the symmetric and antisymmetric transverse states so that $\Psi_{F,s} = (\psi_0 + s\,\psi_1)/\sqrt{2}$.

With the fermion operators at hand we are now in a position to compute the local spectral function related to the tunneling rate of up or down distorted fermions into a point x. The result is again a power law

$$A(E,x) \approx \left(\frac{A_0}{1+e^{x/l}}|E|^{K_\rho} + A_1\, e^{-|x|/l}\right)|E|^{\frac{1}{4K_\rho}-1}. \tag{23}$$

As in the bosonic case, the first term describes the "penetration" of the disorder parameter into the ordered phase near the interface. The second term is the contribution of the Majorana mode. Note, however, that contrary to the bosonic case, here the Majorana mode gives the dominant contribution to the

low-energy tunneling rate near the interface. It is interesting to note that Eq. (23) shows the same leading behavior with E as found in Ref. 14 for tunneling into the edge of the zigzag phase in the weak coupling limit. This is in spite of the very different modeling and physical picture of the edge in the two scenarios. From our analysis it is clear that this behavior stems from a robust zero energy state with topological origin.

VI. NUMERICAL RESULTS

We now turn to a numerical calculation of a concrete microscopic model using DMRG[25] and verify that the long-range correlations are indeed well described by the field theoretical analysis presented above. For this purpose we consider a lattice model which describes similar physics as the original Hamiltonian (2). Specifically we take a model of hard-core bosons on a two-leg ladder at low incommensurate filling [see Fig. 4(a)]:

$$H_{\text{Ladder}} = \sum_{i=1}^{L} \Big[-t_{\parallel} \sum_{a=1,2} (b_{i,a}^{\dagger} b_{i+1,a} + \text{H.c.}) - t_{\perp} (b_{i,1}^{\dagger} b_{i,2} + \text{H.c.}) + \sum_{a=1,2} V_{\parallel} n_{i,a} n_{i+1,a} + V_{\perp} n_{i,1} n_{i,2} \Big], \tag{24}$$

where $b_{i,a}^{\dagger}$ create a (hard-core) boson on site i of leg $a = 1,2$. The two legs of the ladder represent the preferred up and down distortion of a particle. The corresponding Ising variable is the relative density $\hat{\sigma}_i = n_{i,1} - n_{i,2}$. The repulsive interaction $V_{\parallel}$ between particles on the same leg favors a zigzag arrangement to minimize the interaction energy, just as the dipolar interaction does in the original system. At the same time the hopping on a rung $t_{\perp}$ counters that ordering tendency. The latter is directly related to the tunneling matrix element between the two favored states of the rotor $\phi_{\sigma} = 0$ and π. Tuning $t_{\perp}$ to drive the phase transition is analogous to varying the transverse trap frequency in the original model. The hopping $t_{\parallel}$ along the ladder drives the longitudinal quantum fluctuations. At incommensurate filling, just as in the continuum, these fluctuations prevent crystalline order from forming. Finally we fix a large repulsion $V_{\perp}$ ($\gg V_{\parallel}, t_{\parallel}, t_{\perp}$) to suppress double occupation of a rung.

To characterize the ground state we compute the staggered Ising correlation function and string correlation function, which are defined respectively as

$$C_I(r_i - r_j) = \cos(\pi \rho_0 (r_i - r_j)) \langle \hat{\sigma}_i \hat{\sigma}_j \rangle, \qquad C_{\text{str}}(r_i - r_j) = \langle \hat{\sigma}_i e^{i\pi \sum_{l=j}^{i} n_l} \hat{\sigma}_j \rangle. \tag{25}$$

Results of two calculations which differ only by the value of the tuning parameter $t_{\perp}$ are presented in Fig. 4. The lattice size in both cases is $L = 256$ unit cells (rungs), the filling is $\rho_0 \approx 1/3$ per unit cell, and $V_{\parallel} = t_{\parallel} = 1$. The transverse hopping is chosen to be $t_{\perp} = 0.05$ in one calculation [Fig. 4(b)] and $t_{\perp} = 0.8$ in the other [Fig. 4(c)], so that the system is in the zigzag-ordered phase in the first and in the disordered phase in the second calculation. As anticipated, the Ising correlations decay like a power law of distance in the ordered phase while the string correlation saturates to a finite value. When the transverse tunneling is increased to $t_{\perp} = 0.8$ both correlations decay exponentially with distance.

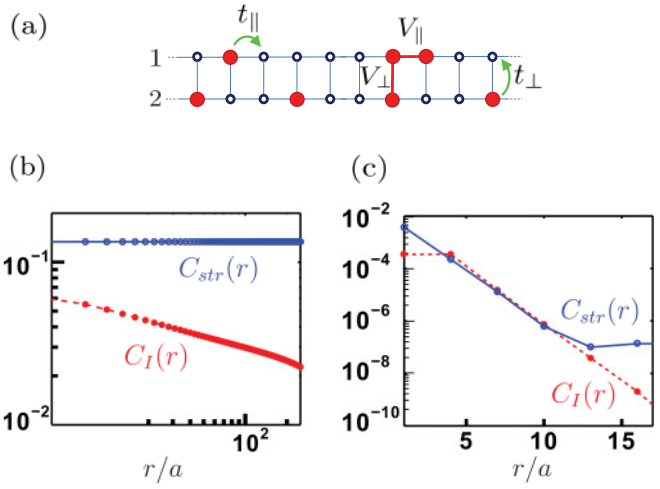

FIG. 4. (Color online) DMRG calculation of correlations in the two-leg ladder model (24). The two legs of the ladder illustrated in panel (a), correspond to the up and down distortion. $V_{\perp}$ is taken to be the largest energy scale to exclude double occupancy of a rung, and the zigzag transition is tuned by varying the ratio $t_{\perp}/V_{\parallel}$. (b) The component with spatial frequency $\pi\rho_0$ of the Ising (red dashed) and string (blue solid) correlation functions in the ordered phase on a log-log plot. The string correlations display true long-range order while the Ising correlations decay as a power law. (c) The same correlation functions calculated in the disordered phase plotted on a log-linear plot, where both are seen to decay exponentially.

VII. CONCLUSION

The zigzag transition observed in chains of trapped ions[7] is a mechanical distortion that occurs when the ion chain is compressed or the transverse confinement decreased beyond a critical point. The transition is well described by a classical theory neglecting all quantum (as well as thermal) fluctuations.[6] In this paper we have shown how the analogous transition takes place in an elongated trap of ultracold dipolar particles, where quantum fluctuations are greatly enhanced compared to the ion system.

Quantum fluctuations are found to have a profound effect on the transition and on the nature of the ordered phase. In particular, the $\mathbb{Z}_2$ symmetry of the system, which is broken in the classical zigzag phase, is restored by the quantum fluctuations of particle positions along the trap. Instead, the quantum zigzag phase is characterized by a nonlocal, Ising string order parameter. We also find zero energy edge states, localized at interfaces between the zigzag phase and the disordered (linear) phase, that are a direct consequence of the nonlocal order in the bulk. It is notable that such nontrivial correlations are found in the most natural setting for polar molecules with no need for special engineering of interactions.

We have calculated the experimental signatures of the edge states that are expected to be seen in tunneling experiments. It would also be interesting to observe the bulk string order directly using *in situ* detection of the particle positions.[26] From the fundamental perspective, our analysis provides another example of a rather rare class of systems which exhibit

topological order (or at least nonlocal string order) in a gapless phase. Other examples in this class include the Haldane phase of spin-3/2 chains and a Haldane liquid phase predicted to occur for two-component dipolar fermions in an optical lattice.[27] The zigzag phase is somewhat special in this class in that it occurs in the presence of full (continuous) translational symmetry rather than in a lattice.

ACKNOWLEDGMENTS

We thank P. Azaria, E. Berg, T. Giamarchi, and A. Vishwanath for helpful discussions. E.A. acknowledges support of the ISF and of the Louis and Ida Rich Career development chair. S.D.H acknowledges support by the Swiss Society of Friends of the Weizmann Institute of Science. E.G.D.T. is supported by the Adams Fellowship Program of the Israel Academy of Sciences and Humanities.

APPENDIX A: RE-FERMIONIZATION OF THE DOUBLE SINE-GORDON MODEL

Here we review the re-fermionization scheme for the double sine-Gordon model[18,19,28](8). Let us start by rewriting the Hamiltonian (8) as follows:

$$\begin{aligned}\mathcal{H}_\sigma = &\frac{u_\sigma}{2\pi}\frac{1+K_\sigma^2}{2K_\sigma}\int dx[(\partial_x\theta_\sigma)^2+(\partial_x\phi_\sigma)^2]\\ &+\frac{u_\sigma}{2\pi}\frac{1-K_\sigma^2}{2K_\sigma}\int dx[-(\partial_x\theta_\sigma)^2+(\partial_x\phi_\sigma)^2]\\ &-\int dx(g_1\cos 2\phi_\sigma + g_2\cos 2\theta_\sigma).\end{aligned} \tag{A1}$$

Using the identities,

$$\sqrt{\rho_0/\pi}:e^{-i(\theta_\sigma-\phi_\sigma)}:\simeq \xi_R^+ + i\,\xi_R^-, \tag{A2}$$

$$\sqrt{\rho_0/\pi}:e^{-i(\theta_\sigma+\phi_\sigma)}:\simeq \xi_L^- + i\,\xi_L^+, \tag{A3}$$

we find that the re-fermionized version of the first and third terms in this Hamiltonian (A1) give the quadratic Majorana model,

$$\mathcal{H}_\sigma^{(0)} = \int dx \sum_{\eta=\pm}\xi^\eta\left[-i\,\frac{\tilde{u}_\sigma}{2}\,\partial_x\tau^z+\Delta_\eta\tau^y\right]\xi^\eta, \tag{A4}$$

where $\xi^\pm=(\xi_R^\pm,\xi_L^\pm)^T$, $\tilde{u}_\sigma = u_\sigma(1+K_\sigma^2)/2K_\sigma$, and $\Delta_\pm = \pi(g_2\pm g_1)/\rho_0$. The re-fermionized version of the second term in Eq. (A1) has the form of an interaction,

$$\mathcal{H}_\sigma^{(I)} = V\int dx\,\xi_R^-\xi_L^+\xi_R^+\xi_L^-, \tag{A5}$$

where $V = 2\pi u_\sigma(1-K_\sigma^2)/2K_\sigma$. As explained in Sec. IV this interaction is irrelevant in the renormalization group sense and therefore not expected to alter the critical properties. It can, however, affect a shift of the critical point from the naive value $\Delta_- = 0$. As explained in the text this shift can be estimated by decoupling the interaction term V so that the renormalized values of Δ_+ and Δ_- become mean-field parameters to be determined self-consistently. If V is small compared to Δ_+ the shift in Δ_- can be easily obtained perturbatively by substituting $\xi_R^+\xi_L^+$ in the interaction term by their expectation value in the unperturbed ground state,

$$-i\langle\xi_R^+\xi_L^+\rangle = \frac{\Delta_+}{\rho_0\tilde{u}_\sigma}\log\left[\frac{\rho_0\tilde{u}_\sigma}{\Delta_+}+\sqrt{\left(\frac{\rho_0\tilde{u}_\sigma}{\Delta_+}\right)^2+1}\right]. \tag{A6}$$

Then the renormalized value of Δ_- is $\tilde{\Delta}_- = \Delta_- - i\langle\xi_R^+\xi_L^+\rangle V$. In the limit $\Delta_+ \gg \rho_0\tilde{u}_\sigma$ this approaches $\tilde{\Delta}_- = \Delta_- + V$.

APPENDIX B: THE MAJORANA EDGE STATE

In this Appendix we solve the Bogoliubov-deGennes (BdG) equations in the presence of an edge and show that there is a single zero energy solution. For simplicity we take a sharp change in the mass term,

$$\Delta_-(x) = \begin{cases}\Delta_0 & x<0 \;\Rightarrow\; \text{disorderd}\\ -\Delta_0 & x>0 \;\Rightarrow\; \text{ordered}\end{cases}. \tag{B1}$$

When $K_\sigma = 1$ the critical point of the Ising model (8) is at $\Delta_- = 0$, therefore, Eq. (B1) defines a boundary between an ordered phase for $x>0$ and a disordered one for $x<0$. The BdG equations for this situation are given by

$$\left[-i\,\frac{u_\sigma}{2}\partial_x\tau^z+\Delta_-(x)\tau^y\right]\chi_E(x) = E\,\chi_E(x), \tag{B2}$$

where $\chi_E(x) = \{u_E(x), v_E(x)\}^{\mathrm{T}}$ is the eigenstate of Eq. (B2) with energy E. The physical solutions of (B2) are at energies above the gap ($E>\Delta_0$) except for the single zero energy solution,

$$\chi_0(x) = \sqrt{\frac{2\Delta_0}{u_\sigma}}e^{-\frac{2\Delta_0}{u_\sigma}|x|}\begin{pmatrix}1\\-1\end{pmatrix}. \tag{B3}$$

The solution of the BdG equations immediately gives us the quasiparticle operators,

$$\gamma_E = \int dx\;[u_E(x)\xi_R(x) - v_E(x)\xi_L(x)], \tag{B4}$$

$$\gamma_E^\dagger = \int dx\,[u_E^*(x)\xi_R(x) - v_E^*(x)\xi_L(x)], \tag{B5}$$

and especially the localized Majorana operator,

$$\gamma_0 = \gamma_0^\dagger = \sqrt{\frac{2\Delta_0}{u_\sigma}}\int dx\;e^{-\frac{2\Delta_0}{u_\sigma}|x|}(\xi_R^- + \xi_L^-). \tag{B6}$$

APPENDIX C: LOW-ENERGY LIMIT FOR FERMIONIC DIPOLES

In case of fermions it is simpler to derive the bosonization identities starting from the weak coupling picture considered in Refs. 10–12. Here we will review the derivation of the low-energy theory in this case and draw analogies to the field theory derived above (8) starting from strongly coupled dipolar particles. Guided by this low-energy theory we will give a phenomenological expression for the field operators.

In Ref. 12 the two lowest sub-bands of the transverse confining potential are considered. The zigzag transition takes place when the chemical potential is placed at the bottom of the second sub-band. At this point the group velocity of

the second sub-band is zero and the bosonization procedure cannot be carried out. However, we can still bosonize the first sub-band. The Hamiltonian of the two sub-bands can be written as follows:

$$H = \frac{u_0}{2\pi}\int dx\left[K(\partial_x\theta_0)^2 + \frac{1}{K}(\partial_x\phi_0)^2\right] + \int dx\,\psi_1^\dagger\left(-\frac{\partial_x^2}{2m}+\delta\right)\psi_1 + \int dx\left[-\frac{g}{\pi}\partial_x\phi_0\psi_1^\dagger\psi_1 + \frac{u_1}{2}(e^{i2\theta_0}\psi_1\partial_x\psi_1 + \text{H.c.})\right], \tag{C1}$$

where δ is the difference between the energy of the second sub-band and the chemical potential, $\delta = \epsilon_1 - \mu$. The field operator ψ_1 belongs to the second sub-band and the first sub-band has been bosonized,

$$\psi_0 = \sum_{r=R,L} \mathrm{U}_r \lim_{\rho_0\to\infty}\sqrt{\frac{\rho_0}{2\pi}}\,e^{\mathrm{i}rk_Fx}e^{-\mathrm{i}(r\phi_0-\theta_0)}, \tag{C2}$$

where U_r is the appropriate Klein factor. The density-density interaction g and the pairing u in the Hamiltonian (C1) originate in the Coulomb interaction.[11]

In order to decouple the pairing term in the Hamiltonian (C1) the authors of Ref. 12 apply the unitary transformation,

$$U = e^{\mathrm{i}\int dx'\,\theta_0\psi_1^\dagger\psi_1}, \tag{C3}$$

such that the transformed operators are given by

$$\tilde{\psi}_0 = U^\dagger\psi_0 U \sim \sum_{r=R,L} e^{irk_Fx}e^{-i(r\phi_0-\theta_0)}e^{-r\frac{i\pi}{2}\int dx'\mathrm{sgn}(x-x')\psi_1^\dagger\psi_1}, \tag{C4}$$

and

$$\tilde{\psi}_1 = U^\dagger\psi_1 U = e^{-i\theta_0}\psi_1. \tag{C5}$$

The Hamiltonian (C1) then assumes the form,

$$H = \frac{u_0}{2\pi}\int dx\left[K(\partial_x\theta_\rho)^2 + \frac{1}{K}(\partial_x\phi_\rho)^2\right] + \int dx\,\xi\left[-\mathrm{i}\frac{u_1}{2}\partial_x\tau^z + 2\delta\,\tau^y\right]\xi - \int dx\,\frac{\lambda}{\pi}\partial_x\phi_\rho\psi_1^\dagger\psi_1\,. \tag{C6}$$

Here the curvature of the second sub-band has been neglected compared to the linear pairing term u. We have also switched the notations here such that $\partial_x\phi_\rho = \partial_x\phi_0 + \pi\psi_1^\dagger\psi_1$ is the fluctuation in the total density, and $\theta_\rho = \theta_0$ is the conjugate phase. We would also like to note that one can recover the Majorana theory (12) by decomposing $\tilde{\psi}_1$ into its real and imaginary parts as follows:

$$\tilde{\psi}_1 = \frac{e^{i\frac{\pi}{4}}}{\sqrt{2}}(\xi_R + i\,\xi_L)\,. \tag{C7}$$

The Hamiltonian (C6),(6),(8) and (9) are identical. They both consist of two sectors, a Luttinger liquid and single nonchiral massive Majorana field. Therefore, we identify our theory as the strong coupling limit of this one.

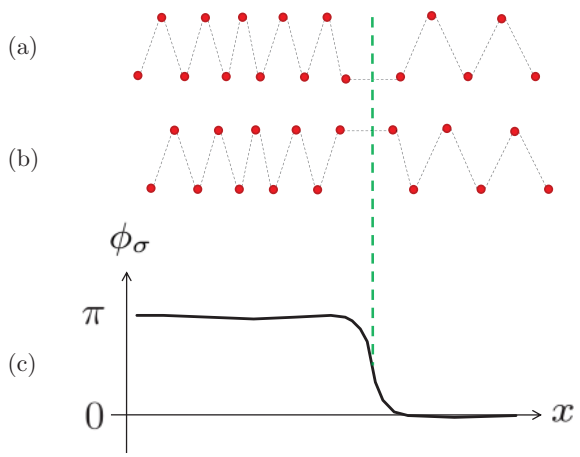

FIG. 5. (Color online) (a) and (b) A chain with a soliton that is created by a defect in the $s = \uparrow$ and $s = \downarrow$ state respectively. (c) In both cases the field ϕ_σ is shifted by $-\pi$ due to the soliton.

Apparently, the expressions for the single-particle operators (C4) and (C5) are sufficient to express the fermion operators in the $s = \uparrow, \downarrow$ state in the zigzag. However, the operator (C4) is written in an inconveniently nonlocal form. We can overcome this inconvenience by replacing (C4) with a phenomenological expression. As shown in Fig. 5 the insertion of a particle both into the $s = \uparrow$ and $s = \downarrow$ states in the zigzag shifts the field ϕ_σ by $\pm\pi$. The operator that shifts ϕ_σ by $\pm\pi$ is $e^{\pm\mathrm{i}\theta_\sigma}$. Therefore, we replace the nonlocal string with θ_σ:

$$\psi_0 \sim \sum_{r=R,L} e^{irk_Fx}e^{-i(r\phi_\rho-\theta_\rho)}e^{ri\theta_\sigma}. \tag{C8}$$

This operator creates a soliton in the σ sector in addition to a plasmonic excitation in the charge sector. Similarly, the operator ψ_1 has the form of a spinon multiplied by the factor $e^{\mathrm{i}\theta_\rho}$ that inserts a charge at zero momentum.

We can now write expressions for second quantized fermion operators inserted to the up and down positions in the tube $s = \uparrow, \downarrow$ as the appropriate superpositions of fermions from the symmetric and antisymmetric sub-bands,

$$\Psi_{F,s} = \frac{1}{\sqrt{2}}(\psi_0 + s\,\psi_1). \tag{C9}$$

APPENDIX D: TUNNELING DOS ON THE EDGE

1. Bosons

The low-energy limit of the second quantized Bose operator is (19)

$$\Psi_{B,s}^\dagger \simeq \beta_0\sqrt{\rho_0}\,e^{-i(\theta_\rho+s\,\theta_\sigma)} + \beta_1\sqrt{\frac{2\pi\,\Delta_0}{u_\sigma}}e^{-\frac{2\Delta_0}{u_\sigma}|x|} \times e^{-i\,\theta_\rho}[e^{i(\phi_\rho+2\pi\rho_0x)} - i\,s\,e^{-i(\phi_\rho+2\pi\rho_0x)}]\gamma_0. \tag{D1}$$

The Bose operator is used to compute the single-particle Green's function in the effective field theory (6) and (8). The contribution of the first term in the Bose operator is found by noting that the disorder parameter $e^{\pm i\theta_\sigma}$ has an expectation value in the disordered side of the interface that penetrates to the ordered side and decays there as $e^{-x/l}$ ($l = \tilde{u}_\sigma/4\Delta_0$ is the

correlation length in the ordered phase). We can therefore replace the operator $e^{\pm i\theta_\sigma}$ by this expectation value. The contribution from the second component of the Bose operator is computed using the form of the zero mode (B3) and the Luttinger liquid which describes the density modes. Putting all this together we have

$$\begin{aligned} G_B(\tau,x) &= -\langle T_\tau \Psi_{B,s}(\tau,x)\Psi^\dagger_{B,s}(0,x)\rangle \\ &\simeq -|\beta_0|^2\,\rho_0\sqrt{\frac{1}{1+2\rho_0 l}}\,\frac{e^{-x/l}}{1+e^{-x/l}}\left(\frac{1}{\rho_0 u_\rho|\tau|}\right)^{\frac{1}{4K_\rho}} \\ &\quad -|\beta_1|^2\,\frac{\pi}{2l}e^{-|x|/l}\left(\frac{1}{\rho_0 u_\rho|\tau|}\right)^{K_\rho+\frac{1}{4K_\rho}}, \end{aligned} \tag{D2}$$

where we have used the fact that

$$\langle T_\tau \gamma_0(\tau)\gamma_0(0)\rangle = \tfrac{1}{2}\mathrm{sgn}(\tau). \tag{D3}$$

To obtain the retarded Green's function we analytically continue the function (D2),

$$\begin{aligned} &G_B(t,x) \\ &= \simeq\Theta(t)\Bigg[\sin\frac{\pi}{8K_\rho}\sqrt{\frac{\rho_0^2}{1+2\rho_0 l}}\,\frac{|\beta_0|^2\,e^{-x/l}}{1+e^{-x/l}}\left(\frac{1}{\rho_0 u_\rho t}\right)^{\frac{1}{4K_\rho}} \\ &\quad +\frac{\pi|\beta_1|^2}{2l}\,\sin\left[\frac{\pi}{2}\left(K_\rho+\frac{1}{4K_\rho}\right)\right]e^{-|x|/l} \\ &\quad \times\left(\frac{1}{\rho_0 u_\rho t}\right)^{K_\rho+\frac{1}{4K_\rho}}\Bigg]., \end{aligned} \tag{D4}$$

The imaginary part of the Fourier transformed version of this function gives the local DOS:

$$A_B(\omega,x) \simeq \frac{B_0\,|\omega|^{\frac{1}{4K_\rho}-1}}{1+e^{x/l}} + B_1\,e^{|x|/l}|\omega|^{K_\rho+\frac{1}{4K_\rho}-1}, \tag{D5}$$

where

$$B_0 \simeq |\beta_0|^2\,\rho_0\sqrt{\frac{\pi/2}{(1+2\rho_0 l)}}\,\frac{1}{\Gamma[1/4K_\rho]}\left(\frac{1}{\rho_0 u_\rho}\right)^{\frac{1}{4K_\rho}},$$

and

$$B_1 \simeq |\beta_1|^2\,\frac{1}{2l}\,\frac{\sqrt{\pi^3/8}}{\Gamma[K_\rho+1/4K_\rho]}\left(\frac{1}{\rho_0 u_\rho}\right)^{K_\rho+\frac{1}{4K_\rho}}.$$

The leading contribution to the local DOS stems from the penetration of the disorder field into the ordered phase. The subleading contribution originates from the Majorana edge state.

2. Fermions

The low-energy limit of the fermion operator was found above and is given by

$$\begin{aligned} \Psi_{F,s} \simeq \frac{1}{\sqrt{2}}\Bigg[&\alpha_0\sum_{r=R,L}\sqrt{\rho_0}e^{i\,r k_F x}e^{-i\,(r\phi_\rho-\theta_\rho)}e^{ri\,\theta_\sigma} \\ &+s\,\alpha_1\,\mathrm{i}\sqrt{\frac{\Delta_0}{4u_\sigma}}e^{i\,\theta_\rho}e^{\frac{u_\sigma}{\Delta_0}|x|}\gamma_0\Bigg]. \end{aligned} \tag{D6}$$

We use this operator in the effective low-energy theory (6) and (8) to obtain the imaginary time Green's function in the same way as discussed above for the bosonic case. This gives

$$\begin{aligned} G_F(\tau,x) \simeq -\mathrm{sgn}(\tau) \\ \times\Bigg[&\frac{|\alpha_0|^2\rho_0}{\sqrt{1+2\rho_0 l}}\,\frac{e^{-x/l}}{1+e^{-x/l}}\left(\frac{1}{\rho_0 u_\rho|\tau|}\right)^{K_\rho+\frac{1}{4K_\rho}} \\ &+|\alpha_1|^2\,\frac{\pi}{2l}e^{-|x|/l}\left(\frac{1}{\rho_0 u_\rho|\tau|}\right)^{\frac{1}{4K_\rho}}\Bigg]. \end{aligned} \tag{D7}$$

To obtain the low-energy local DOS we analytically continue this expression and the imaginary part in Fourier space,

$$A_F(\omega,x) \simeq \frac{A_0\,|\omega|^{K_\rho+\frac{1}{4K_\rho}-1}}{1+e^{x/l}} + A_1\,e^{|x|/l}|\omega|^{\frac{1}{4K_\rho}-1}, \tag{D8}$$

where

$$A_0 \simeq |\alpha_0|^2\rho_0\sqrt{\frac{1}{1+2\rho_0 l}}\,\frac{\sqrt{\pi/2}}{\Gamma[K_\rho+1/4K_\rho]}\left(\frac{1}{\rho_0 u_\rho}\right)^{K_\rho+\frac{1}{4K_\rho}},$$

and

$$A_1 \simeq |\alpha_1|^2\,\frac{1}{2l}\,\frac{\sqrt{\pi^3/8}}{\Gamma[1/4K_\rho]}\left(\frac{1}{\rho_0 u_\rho}\right)^{\frac{1}{4K_\rho}}.$$

In this case the leading contribution comes from the localized Majorana fermion, and the subleading one stems from the penetration of the disorder parameter into the ordered phase.

[1] T. Lahaye, T. Koch, B. Fröhlich, M. Fattori, J. Metz, A. Griesmaier, S. Giovanazzi, and T. Pfau, Nature (London) **448**, 672 (2007).

[2] K.-K. Ni, S. Ospelkaus, M. H. G. de Miranda, A. Pe'er, B. Neyenhuis, J. J. Zirbel, S. Kotochigova, P. S. Julienne, D. S. Jin, and J. Ye, Science (NY) **322**, 231 (2008).

[3] G. Pupillo, A. Micheli, M. Boninsegni, I. Lesanovsky, and P. Zoller, Phys. Rev. Lett. **104**, 223002 (2010).

[4] E. G. Dalla Torre, E. Berg, and E. Altman, Phys. Rev. Lett. **97**, 260401 (2006).

[5] N. R. Cooper and G. V. Shlyapnikov, Phys. Rev. Lett. **103**, 155302 (2009).

[6] S. Fishman, G. De Chiara, T. Calarco, and G. Morigi, Phys. Rev. B **77**, 064111 (2008).

[7] G. Birkl, S. Kassner, and H. Walther, Nature (London) **357**, 310 (1992).

[8] E. Shimshoni, G. Morigi, and S. Fishman, Phys. Rev. Lett. **106**, 010401 (2011).

[9] E. Shimshoni, G. Morigi, and S. Fishman, Phys. Rev. A **83**, 032308 (2011).

[10]J. S. Meyer, K. A. Matveev, and A. I. Larkin, Phys. Rev. Lett. **98**, 126404 (2007).
[11]J. S. Meyer and K. A. Matveev, J. Phys. Condens. Matter **21**, 023203 (2009).
[12]M. Sitte, A. Rosch, J. S. Meyer, K. A. Matveev, and M. Garst, Phys. Rev. Lett. **102**, 176404 (2009).
[13]E. Orignac and T. Giamarchi, Phys. Rev. B **57**, 11713 (1998).
[14]O. A. Starykh, D. L. Maslov, W. Häusler, and L. I. Glazman, in *Interactions and Quantum Transport Properties of Lower Dimensional Systems*, Springer Lecture Notes in Physics Vol. 544, edited by T. Brandes (Springer, New York, 2000), p. 37.
[15]E. Orignac and T. Giamarchi, Phys. Rev. B **56**, 7167 (1997).
[16]G. E. Astrakharchik, G. De Chiara, G. Morigi, and J. Boronat, J. Phys. B **42**, 154026 (2009).
[17]K. A. Matveev, Phys. Rev. B **70**, 245319 (2004).
[18]D. G. Shelton, A. A. Nersesyan, and A. M. Tsvelik, Phys. Rev. B **53**, 8521 (1996).
[19]P. Lecheminant, A. O. Gogolin, and A. A. Nersesyan, Nucl. Phys. B **639**, 502 (2002).
[20]J. B. Zuber and C. Itzykson, Phys. Rev. D **15**, 2875 (1977).
[21]A. Y. Kitaev, Phys. Usp. **44**, 131 (2001).
[22]C. Kollath, M. Köhl, and T. Giamarchi, Phys. Rev. A **76**, 063602 (2007).
[23]W. S. Bakr, A. Peng, M. E. Tai, R. Ma, J. Simon, J. I. Gillen, S. Fölling, L. Pollet, and M. Greiner, Science (NY) **329**, 547 (2010).
[24]J. F. Sherson, C. Weitenberg, M. Endres, M. Cheneau, I. Bloch, and S. Kuhr, Nature (London) **467**, 68 (2010).
[25]S. R. White, Phys. Rev. Lett. **69**, 2863 (1992).
[26]M. Endres, M. Cheneau, T. Fukuhara, C. Weitenberg, P. Schauß, C. Gross, L. Mazza, M. C. Bañuls, L. Pollet, I. Bloch *et al*., Science **334**, 200 (2011).
[27]J. P. Kestner, B. Wang, J. D. Sau, and S. Das Sarma, Phys. Rev. B **83**, 174409 (2011).
[28]Readers who seek general information regarding the re-fermionization procedure may consult, e.g., Refs. 29 or 30.
[29]T. Giamarchi, *Quantum Phyiscs in One Dimension* (Oxford Science Publications, Oxford, 2003).
[30]A. O. Gogoglin, A. A. Nersesyan, and A. M. Tsvelik, *Bosonization Approach to Strongly Correlated Systems* (Cambridge University Press, Cambridge, 1998).